Even-Odd effects in the electrical conductance of a three terminals device composed by linear chains: an analytical approach.

[a] Moreira, A.C.L*; L. S. Marques[b]

[a] Núcleo Interdisciplinar em Ciências Exatas e da Natureza - NICEN

Universidade Federal de Pernambuco, 50740-540, Recife/PE, Brasil;

[b] Centro de Física das Universidades do Minho e do Porto,
Universidade do Minho, 4710-057, Braga, Portugal

*Corresponding author: aclm.ufpe@gmail.com

Abstract

In this work we propose a theoretical study of odd-even effects in charge transport through a linear three terminal chain device. We use the Landauer approach, with the electronic structure treated at tight binding (TB) level and model the self-energy as an energy independent parameter. Moreover, we use decimation techniques to renormalize the system, reducing it into a 3x3 matrix, so as to make an analytical treatment. By varying the size of the chain, we alter not only the parity of the full system but also the parity of each possible pathway and show how odd-even effect appears in the transmission function, local density of states and the behavior of the electrical current as function of the parity. Our theoretical approach reveals, in a clear way, how the parity of each branch competes with the parity of the full system to the conductance values near the Fermi level.

Keywords: Quantum transport, Three terminal device, Linear chain.

1. INTRODUCTION

A single molecule working as an active electronic component in an integrated circuit, in principle, must be the smallest size for miniaturization of an electronic device. One of the first proposals in this sense, was done by Aviram and Ratner [1] where, it was shown that an asymmetric molecule could act as a molecular rectifier. Since then, the field of molecular electronics gained a lot of interest and nowadays, with advanced experimental techniques, this field became a potential candidate to substitute silicon-based devices [2]. Thus, understanding the behavior of molecular devices, is a necessary step to control its electric charge flux.

One of the most intriguing phenomena at molecular scale are the odd-even effects [3–10]. This phenomenon involves a drastic change of the electrical conductance of a molecular device as function of the number of atoms (odd or even) acting as bridge between two moieties of a given system. In general, these changes can be associated to geometrical features [5,8] or to the local density of states [3,4,10–12] (LDOS) behavior of the system. An example of a drastic change in the electrical conductance involving geometrical features, is reported by Toledano and coworkers [8]. In this work, experiments were carried out with a system composed by a phenyl ring attached to a methylenic bridge connected to a silicon surface and a caping lead surface above the phenyl. They observed that, at low temperatures, for ethyl (n=2, CH_2 groups) and butyl ($n=4$) bridges the current density is greater than for propyl (n=3) and pentyl (n=5) ones. This apparent contradiction between butyl and propyl, with the exponential decay law of conductance for increasing lengths of the methylenic bridges, is due to the different orientation of the phenyl ring as function of the odd/even number of carbons in the bridge. Thus, while for even bridges the orientation is such that the overlap between the lead molecule and substrate increases, for odd bridges this overlap decreases. Furthermore, this inversion between butyl and propyl is not observed at room temperature (300 K).

An experimental example of a LDOS behavior as function of even/odd atoms in an atomic wire can be found in Smit *et al* [12], where the authors used a scanning tunnel microscope (STM) and mechanically controllable break junctions (MCBJ) atomic contacts to form atomic wires with gold (Au), platinum (Pt) and iridium (Ir). They observed an oscillatory evolution of conductance during the formation of the monoatomic chain as function of odd/even number of atoms. This parity oscillation is well pronounced for Au chains and, despite less evident for Pt and Ir chains, this parity is also observed for these atoms, permitting to conclude that this is a universal feature of metallic atomic wires. We stress here that the parity oscillation is not restrict to metallic wires, as reported by Whitesides *et al* [6]. In this work, the authors compare charge transport across self-assembled monolayers (SAMs) of n-alkanethiols containing odd and even numbers of methylenes and observed that both types of n-alkanethiols exhibit the expected exponential decrease in current density with the number of methylenes, however, alkanethiols with an even number of methylenes show higher transmission than the alkanethiols with an odd number of methylenes. The above experimental data, triggered

off a lot of theoretical works as an attempt to explain these results [3,5,7,10,11]. With the aid of the Friedel sum rule, Sim *et al* [3] perform first-principles calculations of conductance through monatomic sodium wires. The authors concluded that a wire containing an odd number of atoms has a higher LDOS near the Fermi level, with transmission's peaks near the unity. An opposite behavior occurs for systems with an even number of atoms thus, explaining the transmission's valley near the Fermi level. We stress here that for a two terminal linear chain device (2T-device), this essential result, can be obtained by simple tight binding approaches as reported by some authors [2,13], i.e.: chains with an odd [even] number of sites have a peak [valley] in the transmission function at the Fermi energy.

Similar results were obtained for even-odd methylenic bridges attached to graphene electrodes[7] – using non equilibrium Green´s function (NEGF) with density functional tight binding (DFTB) calculations – and using density functional theory (DFT) again, with NEGF[10]. The main result of these theoretical works can be summarized as follows: if there is an alignment between the Fermi level and a level in the atomic wire spectrum for the system studied, there will be a peak transmission at this energy value. In some works [7,10], for example, this alignment occurs for odd methylenic bridges, generating a peak in the transmission at the Fermi level position and an opposite behavior for even methylenic bridges: a valley in the transmission. Note that, the key point is the energy alignment between the wire's spectrum and the Fermi level. Thus, changing the position of the Fermi level – by altering the material of the contacts, for example – the even/odd conductance behavior as previous discussed, can change.

In the analysis of the previous paragraphs, a question that naturally emerge is: how even-odd effects appears in atomic wires composed by three terminal's devices? Note that for this kind of device, there are many possible configurations. In a tight binding approach, for example, a system can have an even number of sites but the effective pathway – from a specific terminal to another – can have an odd number of sites, with odd [even] systems have a peak [valley] in the transmission function when $E=E_F$. However, how the even-odd effects may appear for a given configuration as depicted in figure 1, is still an open question.

This work aims to understand how the even-odd effects may affect the behavior of the transmission function of three terminal systems depicted in figure 1. In special, we will be interested in the transmission near the Fermi level, in the zero-temperature limit [2,14]. To do this, we will make an analytical study of coherent quantum transport, using decimation techniques [15–17] in a tight binding approach together with an energy independent model of the self-energy[18,19], so as to reduce the systems into a renormalized three terminal sites. In what follows, in section 2 we will discuss the characteristics of the models showed in Fig. 1, in section 3 we will present the used formalism, in section 4 we will discuss the results and, finally, in section 5 we will make the conclusions and perspectives.

2. THE MODEL SYSTEMS

The model systems are depicted in figure 1. These systems are linear chains with a bifurcation, changing the systems into a three terminals device. We have six systems that

are basically divided in two groups with each one containing three molecules. In the first group, the molecules have an even number of atoms, denominated by *Ea*, with *a* = 1- 3. In the second one, the molecules have an odd number of atoms denominated by *Oa* with *a* = 1, 2 and 3. These groups are showed in the first (even systems) and second (odd systems) columns of Fig. 1, respectively.

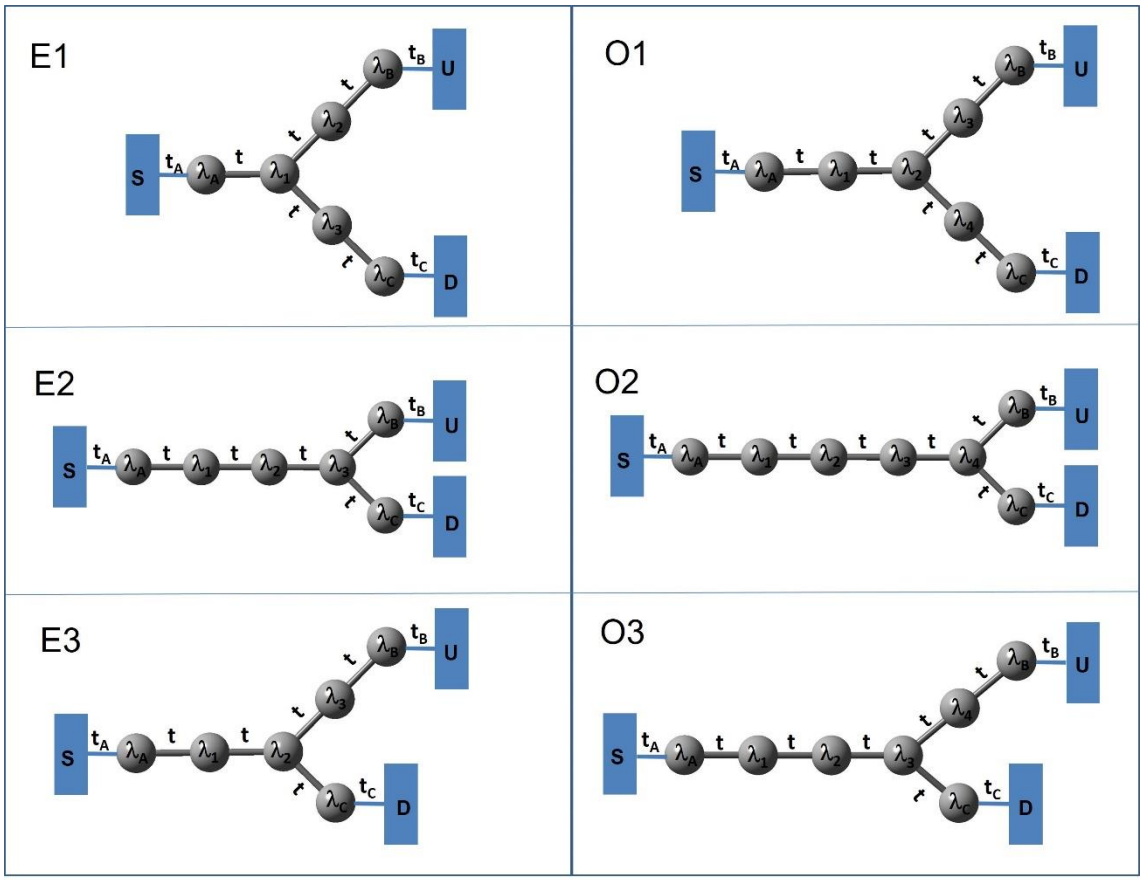

Figure 1: Model systems composed by a three terminal linear chain. Left column contains symmetric (E1 and E2) and asymmetric (E3) systems with even number of atoms (sites) and the right column symmetric (O1 and O2) and asymmetric (O3) systems with odd number of atoms (sites).

IN the case of systems, here called: *E1*, *E2* and *E3*, despite having an even number of atoms there are some crucial differences between them that will interfere in their electrical transport properties. For example, the system *E1* has an even number of sites on each ramification in such a way that a particle that leaves the *S*-contact must cross four sites until arrive at the *U*-contact or the *D*-contact. Things are quite different for system *E2*, despite the total number of atoms of this system is even, each pathway (ramification) has an odd number of sites. Finally, different from *E1* and *E2*, where both pathways are symmetric, the system *E3* is fully asymmetric, i.e., the pathway *S*-*U* (from contact *S* to the contact *U*) has an odd number of sites while the pathway *S*-*D* (from contact *S* to the contact *D*) has an even number of sites. Also, note that for system *E3* the pathway *S*-*U* has more sites to be crossed (five sites) than the pathway *S*-*D* (four sites) Thus, if for systems *E1* and *E2*, a symmetric transmission in each ramification is expected, for *E3* one

might expect an asymmetric transmission with different electrical currents for each pathway.

The analysis for the three odd systems (here called *O1*, *O2* and *O3*) is quite similar. The key point of the system *O1* is that not only the total number of atoms but also each pathway (ramification) has odd number of atoms. Thus, a particle that leaves the *S*-contact must cross five sites until arrive at the *U*-contact or at the *D*-contact. For system *O2* we have an odd number of sites (seven) in the molecule, but an even number of sites on each ramification. Finally, we have the asymmetric system *O3* where the pathway *S*-*U* (from contact *S* to the contact *U*) has an odd number of sites while the pathway *S*-*D* (from contact *S* to the contact *D*) has an even number of sites. It is thus expecting an asymmetric transmission in system O3 with different electrical currents for each pathway.

3. THEORY

A straightforward method to calculate spatially resolved features in quantum transport theory through a linear chain described by a nearest neighbor tight-binding approximation, consists in using Landauer-Büttiker formalism based on Green´s function techniques together with a real-space renormalization approach, the so called, decimation procedure [15,17,19,20]. In this approach, a three terminal linear chain can be transformed into three effective sites, each one with a renormalized on-site energy and with an effective inter-site coupling as showed in figure 2 for system *E1*. This procedure permits us to reduce the degrees of freedom of the system, into a set of nonlinear equations, that makes possible to obtain an analytical version of the (renormalized) Green´s function [16,17]. As a consequence, all quantities that can be calculated with the Green´s function, such as the local density of states (LDOS), the transmission function and so on, become straightforward [17].

We stress here that, although this approach seems to be too simplistic to explain realistic quantum circuits, it has proven to provide good qualitative insights to understand the essential electronic and transport properties of a lot of systems.

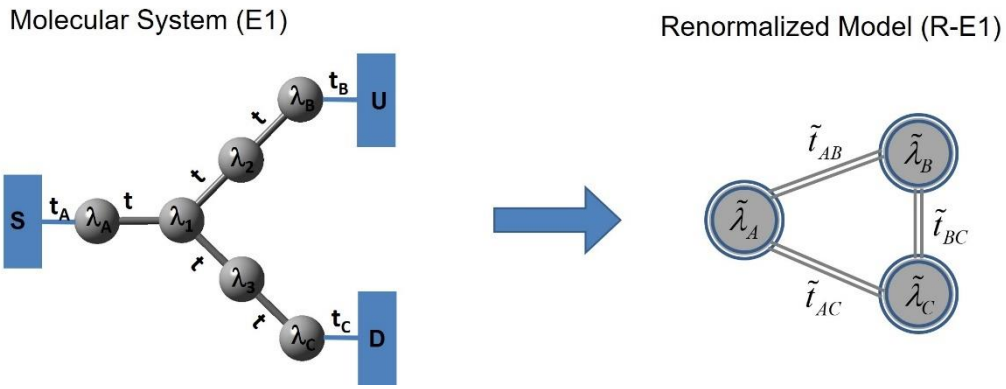

Figure 2: An example of a system (left) and the representation of its renormalized version (right). Note that tilde above the parameters, means a renormalized quantity.

3.1 Formalism

As depicted in Fig. 02 (see also Fig. 01), 'sites' *S, U* and *D* represents the *S*ource contact, *U*pper drain contact and the *D*own drain contact, respectively. These semi-infinite contacts are connected to a *M*olecule composed by a three terminal linear chain in such a way that contacts (*S, U, D*) are, respectively, connected to sites (*A, B, C*) with onsite energies (λ_A, λ_B, λ_C) via tight binding parameters t_A, t_B and t_C. All others internal (molecular) sites have onsite parameter $\lambda_i = \lambda_0$ for i = 1 to N (N = 3 for even systems and N = 4 for odd systems) and hopping parameter t as showed in Fig. 1. In general, the tight binding Hamiltonian of these systems can be written as:

$$\hat{H} = \hat{H}_M + \hat{H}_S + \hat{H}_U + \hat{H}_D + \hat{V} \quad , \tag{1}$$

where the molecular ($\hat{H}_M$), contacts ($\hat{H}_C = \hat{H}_S + \hat{H}_U + \hat{H}_D$) and contact-molecule ($\hat{V}$) part of the Hamiltonian are given by:

$$\hat{H}_M = \sum_{X=A,B,C} \lambda_X \, \hat{c}_X^\dagger \hat{c}_X + \lambda_0 \sum_i \hat{c}_i^\dagger \hat{c}_i + t \sum_{\langle i,j \rangle} \left(\hat{c}_i^\dagger \hat{c}_j + \hat{c}_j^\dagger \hat{c}_i \right) \tag{2}$$

$$\hat{H}_C = \hat{H}_S + \hat{H}_U + \hat{H}_D = \sum_{S=1}^{\infty} E_S \, \hat{d}_S^\dagger \hat{d}_S + \sum_{U=1}^{\infty} E_U \, \hat{d}_U^\dagger \hat{d}_U + \sum_{D=1}^{\infty} E_D \, \hat{d}_D^\dagger \hat{d}_D \tag{3}$$

$$\hat{V} = \sum_S t_A \left(\hat{d}_S^\dagger \hat{c}_A + \hat{c}_A^\dagger \, \hat{d}_S \right) + \sum_U t_B \left(\hat{d}_U^\dagger \hat{c}_B + \hat{c}_B^\dagger \, \hat{d}_U \right) + \sum_D t_C \left(\hat{d}_D^\dagger \hat{c}_C + \hat{c}_D^\dagger \, \hat{d}_C \right) \quad . \tag{4}$$

Due to the coupling of the molecule with the semi-infinite systems, the full system (i.e., the molecule plus semi-infinite contacts) evolves accordingly to an effective Hamiltonian $\tilde{H}_M \to \tilde{H}_M^{eff} = \tilde{H}_0 + \sum_X \tilde{\Sigma}_X^r(E)$ with $\tilde{\Sigma}_X^r(E) = \tilde{\Delta}_X(E) - i\tilde{\Gamma}_X(E)$ the retarded self-energy due to the coupling between the molecule and the semi-infinity contact [21] at site X (X = *A, B, C*). The imaginary terms are given by $\tilde{\Gamma}_X(E) = -2\,\mathrm{Im}[\tilde{\Sigma}_X^r(E)]$ and the real one given by $\tilde{\Delta}_X(E) = \mathrm{Re}[\tilde{\Sigma}_X^r(E)]$. Note that while the real part of the self-energy shifts the level λ_X, the imaginary part is associated with the broadening and finite lifetime of this level [22,23].

Thus, the net effect of coupling the finite system to semi-infinity contacts is a renormalized site energy given by: $\lambda_X^{eff} = \lambda_X + \Sigma_X(E)$, with X = *A, B* and *C*. For simplicity, in this work we will model the self-energy as purely imaginary and energy-

independent parameter[16,19], $\Sigma_X(E) = -i\Gamma_X$, at weak coupling regime[19,24] ($\Gamma_X < t$). With these considerations, the effective molecular Hamiltonian ($\hat{H}_M^{eff}$) can be written as:

$$\hat{H}_M^{eff} = \sum_{X=A,B,C} \left(\lambda_X - i\Gamma_X\right)\hat{c}_X^{\dagger}\hat{c}_X + \sum_i \lambda_i \hat{c}_i^{\dagger}\hat{c}_i + t\sum_{\langle i,j\rangle}\left(\hat{c}_i^{\dagger}\hat{c}_j + \hat{c}_j^{\dagger}\hat{c}_i\right) \quad , \tag{5}$$

where $\langle i, j\rangle$ means that only first neighborhood's interaction for t is non null, as usual in tight binding approaches. Note that in our purely imaginary and energy-independent self-energy model, we have $\lambda_X^{eff} = \lambda_X - i\Gamma_X$.

Once included the contacts effect via a constant self-energy approximation, next step consists in decimate the systems, to bring them into renormalized models that can be treated analytically. Tables 1 and 2 shows the renormalized on-sites energies ($\tilde{\lambda}_X$ with *X = A, B, C*) and the effective couplings ($\tilde{t}_{XY}$ with *X, Y = A, B, C* and $X \neq Y$), for even and odd systems, respectively. All results are written in terms of $\beta \equiv \beta(E)$ given by $\beta \equiv \beta(E) = t(E - \lambda_0 - i\eta)^{-1}$ and $D_Y = \left[1 - \beta^2\left(D_{Y-1}\right)^{-1}\right]$, with *Y = 1, 2* or *3*, $D_0 = 1$ and η an infinitesimal positive number.

Table 1: Renormalized Parameters for Even Systems

System E1
$\tilde{\lambda}_A = \lambda_A - i\Gamma_A + \dfrac{t\beta}{D_1 - \beta^2}$ and $\tilde{\lambda}_X = \lambda_X - i\Gamma_X + t\beta\left(1 + \dfrac{\beta^2}{D_1 - \beta^2}\right)$, with $X = B, C$
$\tilde{t}_{AB} = \tilde{t}_{BA} = \tilde{t}_{AC} = \tilde{t}_{CA} = \dfrac{t\beta^2}{D_1 - \beta^2}$ and $\tilde{t}_{BC} = \tilde{t}_{CB} = \dfrac{t\beta^3}{D_1 - \beta^2}$
System E2
$\tilde{\lambda}_X = \lambda_X - i\Gamma_X + t\beta\left(1 + \dfrac{\beta^2}{D_1 - \beta^2}\right)$, with $X = A, B, C$
$\tilde{t}_{AB} = \tilde{t}_{BA} = \tilde{t}_{AC} = \tilde{t}_{CA} = \dfrac{t\beta^3}{D_1 - \beta^2}$ and $\tilde{t}_{BC} = \tilde{t}_{CB} = t\beta\left(1 + \dfrac{\beta^2}{D_1 - \beta^2}\right)$
System E3
$\tilde{\lambda}_C = \lambda_C - i\Gamma_C + \dfrac{t\beta}{D_1 - \beta^2}$ and $\tilde{\lambda}_X = \lambda_X - i\Gamma_X + t\beta\left(1 + \dfrac{\beta^2}{D_1^2 - \beta^2}\right)$, with $X = A, B$

$\tilde{t}_{AB} = \tilde{t}_{BA} = \dfrac{t\beta^3}{D_1 - \beta^2}$ and $\tilde{t}_{BC} = \tilde{t}_{CB} = \tilde{t}_{AC} = \tilde{t}_{CA} = \dfrac{t\beta^2}{D_1 - \beta^2}$

Table 2: Renormalized Parameters for Odd Systems
System O1
$\tilde{\lambda}_X = \lambda_X - i\Gamma_X + t\beta\left(1 + \dfrac{\beta^2}{D_1 - 2\beta^2}\right)$, with $X = A, B, C$
$\tilde{t}_{AB} = \tilde{t}_{BA} = \tilde{t}_{AC} = \tilde{t}_{CA} = \tilde{t}_{BC} = \tilde{t}_{CB} = \dfrac{t\beta^3}{D_1 - 2\beta^2}$
System O2
$\tilde{\lambda}_X = \lambda_X - i\Gamma_X + \dfrac{t\beta}{D_3}$, with $X = A, B, C$
$\tilde{t}_{AB} = \tilde{t}_{BA} = \tilde{t}_{AC} = \tilde{t}_{CA} = \dfrac{t\beta^4}{D_1 D_2 D_3}$ and $\tilde{t}_{BC} = \tilde{t}_{CB} = \dfrac{t\beta}{D_3}$
System O3
$\tilde{\lambda}_C = \lambda_C - i\Gamma_C + \dfrac{t\beta D_1}{D_1^2 - \beta^2}$ and $\tilde{\lambda}_X = \lambda_X - i\Gamma_X + \dfrac{t\beta\left(1 - 2\beta^2\right)}{D_1^2 - \beta^2}$, with $X = A$, B
$\tilde{t}_{AB} = \tilde{t}_{BA} = \dfrac{t\beta^4}{D_1^2 - \beta^2}$, $\tilde{t}_{AC} = \tilde{t}_{CA} = \dfrac{t\beta^3}{D_1^2 - \beta^2}$ and $\tilde{t}_{BC} = \tilde{t}_{CB} = \dfrac{t\beta^2 D_1}{D_1^2 - \beta^2}$

Once the effective couplings and the renormalized energies of sites A, B and C were obtained the renormalized effective Device Hamiltonian ($\tilde{H}^{eff}_{re-D}$), in a matrix form, can be written as:

$$\tilde{H}^{eff}_{re-D} = \begin{pmatrix} \tilde{\lambda}_A & \tilde{t}_{AB} & \tilde{t}_{AC} \\ \tilde{t}_{BA} & \tilde{\lambda}_B & \tilde{t}_{BC} \\ \tilde{t}_{CA} & \tilde{t}_{CB} & \tilde{\lambda}_C \end{pmatrix} \quad , \tag{6}$$

and the renormalized Green´s function can be calculated inverting a simple 3x3 matrix, i.e.:

$$\tilde{G}^{r}(E)=\begin{pmatrix}\tilde{G}^{r}_{AA}(E) & \tilde{G}^{r}_{AB}(E) & \tilde{G}^{r}_{AC}(E)\\ \tilde{G}^{r}_{BA}(E) & \tilde{G}^{r}_{BB}(E) & \tilde{G}^{r}_{BC}(E)\\ \tilde{G}^{r}_{CA}(E) & \tilde{G}^{r}_{CB}(E) & \tilde{G}^{r}_{CC}(E)\end{pmatrix}=\begin{pmatrix}E-\tilde{\lambda}_{A} & -\tilde{t}_{AB} & -\tilde{t}_{AC}\\ -\tilde{t}_{BA} & E-\tilde{\lambda}_{B} & -\tilde{t}_{BC}\\ -\tilde{t}_{CA} & -\tilde{t}_{CB} & E-\tilde{\lambda}_{C}\end{pmatrix}^{-1} . \quad (7)$$

Note that, in all models, although there is no direct coupling between sites B and C, once decimated the full system into three sites only, an indirect (effective) coupling between sites B and C ($\tilde{t}_{BC}$) naturally appears in the effective Hamiltonian. Within the Green´s function, the transmission function (and thus the electrical current) from terminal *X* to terminal *Y*, in scattering theory, can be expressed as [2,22,25]:

$$T_{XY}(E)=\tilde{\Gamma}_{Y}(E)\,\tilde{\Gamma}_{X}(E)\left|\tilde{G}^{r}_{XY}(E)\right|^{2} \quad . \quad (8)$$

The term $\tilde{\Gamma}_{X}$ ($\tilde{\Gamma}_{Y}$) is the spectral function densities (the imaginary part of the self-energy) due to the coupling with *X*- (Y) contact as previous discussed and $\tilde{G}^{r}_{XY}$ is the retarded Green´s function which can be viewed as the probability for a particle to propagate along the device starting from *X*-contact (*X* = *A*) until the *Y*-contact (*Y* = *B* or *C*). Note that once the system was decimated and reduced to a simple 3x3 matrix, the Green's function can be determined analytically for each case. Finally, with the transmission function of Eq. 8, the electrical current can be calculated as [26]:

$$I_{XY}=\frac{2e}{h}\int_{-\infty}^{+\infty}T_{XY}(E)\left(f_{X}(E)-f_{Y}(E)\right)dE \quad . \quad (9)$$

In Eq. (9) $f_{X}(E)$ is the Fermi distribution function of the *X*-contact and $T_{XY}(E)$ is the transmission function that describes the probability that a particle crosses the system starting from the *X*-lead to the *Y*-lead as defined above. Reminding that for a multi-terminal device, the reflection probabilities are related to the transmission probabilities by the equation $R_{YY}+\sum_{X(\neq Y)}T_{XY}=1$, that is nothing but an electrical current conservation condition [26, 24]. With this basic formalism, we can understand some qualitative features of the systems, as we will show in the next section.

4. RESULTS

Without loss of generality, we will consider the imaginary part as a constant and a symmetric coupling in all three terminals, i.e., $\Gamma_X = \Gamma$, for *X* = *A*, *B* and *C* and adopt Γ = 0.1 eV [23]. Also, we will consider *t* =1 eV and the site energy and the Fermi energy equal zero, $\lambda_X = E_F$ = 0 eV (*X* = *A*, *B*, *C*, 1, 2, 3, 4), due to the inherent electron-hole symmetry of the model with a single electron per site [15]. Furthermore, to get a better understand of the transmission function (T(E)) for each studied system, we also plotted

the local density of states (LDOS) given by[20] $\tilde{\rho}_X(E) = -\pi^{-1}\,\mathrm{Im}(\tilde{G}^r_{XX}(E))$, for each renormalized end-site (*A*, *B* and *C*) and, for the sake of simplicity, we will analyze even and odd cases separately.

4.1 Even systems

Reminding that if a simple tight binding model with one electron per site for a two-terminal device (2T-device) was adopted, then the Fermi level (E_F) coincides with the onsite energy ($E_F = \lambda_0$). In this case, systems with an even number of sites have a valley in the transmission function when $E = E_F = \lambda_0$. With this in mind, we can see in the left upper panel of figure 3 that for the system E1, a valley in the transmission function for $E=0$ occurs for both pathways, i.e., for T_{AB} (red/full line) and for T_{AC} (black circles), as expected. This system is symmetric, in the sense that the upper and the lower pathways are equal and thus we must have $T_{AB}(E) = T_{AC}(E)$, as it should be. Note that system E1, has not only an even number of total sites (six sites) but also an even number of sites on each possible pathway. Also note that we have six eigenvalues but only four peaks in the transmission function. This feature can be understood analyzing the LDOS (lower left panel of Fig. 3) of the system E1, where there is an absence of a state localized in site *A*, around $E = \pm 1$ eV, as showed by the red/full line. As a consequence, these two eigenvalues (around $E = \pm 1$ eV) are forbidden as transport channels. Thus, an even three terminal system (3T-system) with two even branches, behaves like a two-terminal system (2T-system) containing the same number of sites of each branch of the 3T-system.

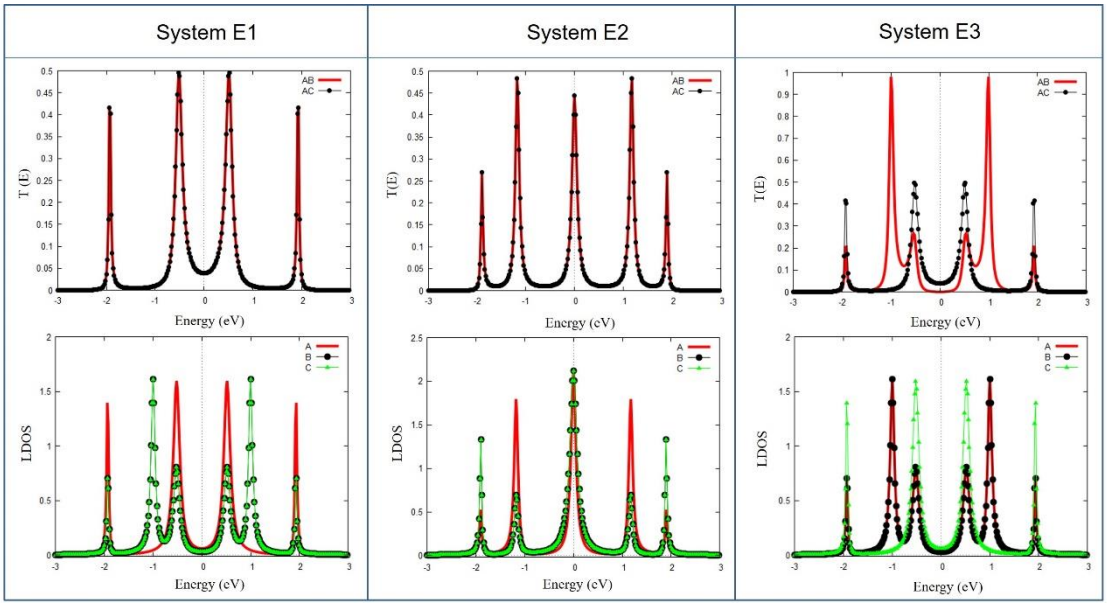

Figure 3: Transmission (upper panels) and LDOS (lower panels) for the three studied even systems. For transmission (upper panels), red/full line is the transmission from site A to site B and the black circles, the transmission from site A to site C. For LDOS (lower panels) we have: red line, black circles and green triangles as the LDOS curves in sites A, B and C, respectively.

For system E2, things are somewhat different and a peak in the transmission function can be observed at $E = 0$ eV as showed in the upper central panel of Fig. 3. This system

has a total of six sites and, once more, is symmetric, in the sense that the upper and the lower pathway are equal with both pathways having an odd number of sites. The behavior of the transmission function can be understood analyzing the LDOS (lower panel) of the system E2: due to the symmetric characteristic of this system, two spatially delocalized degenerate states appear around $E = 0$ eV, as shown in the central lower panel of Fig. 3. These two degenerates and delocalized eigenvalues work as transport channels through both pathways in a symmetric manner and thus we have $T_{AB}(E) = T_{AC}(E)$ as it should be. We stress that, even for an even number of sites in system E2, a peak transmission at $E = E_F = 0$ eV exists for this system. Thus, an even symmetrical 3T-system with two odd branches, behaves like a 2T-system containing the same number of sites in each 3T-branch (five sites for the E2-case).

Finally, we have the system E3. This is an asymmetric system, in the sense that each pathway has a different number of sites. This difference between the upper and the lower pathways, brings an asymmetric behavior in the transmission function different from E1 and E2 systems, in this case we have $T_{AB}(E) \neq T_{AC}(E)$, as showed by the full red line and the black circles in the upper right panel of figure 3. Note that, if for the lower pathway (with an even number of sites) a valley in the transmission function for $E = E_F = 0$ eV is expected, the absence of a peak in the transmission at $E = E_F = 0$ eV for the upper pathway containing an odd number of sites, in principle, should not occur, by analogy with system E2. However, let's remind that system E2 has a very peculiar situation: even number for the total of sites, with symmetrical branches containing an odd number of sites. This combination brings a degenerate state at $E = E_F$. However, this is not the case for system E3 where the asymmetric feature of the system forbids these pair of degenerate eigenvalues at the Fermi level position. This explains the absence of a peak at $E = E_F$ for the upper branch, even if this pathway has an odd number of sites. Another point that should be mentioned refers to the difference in the number of transport channels between the upper and the lower pathways: six channels for the pathway containing five sites (upper branch) as showed by the red/full line and only four channels for the lower pathway with four sites. Once more, this difference can be explained by the LDOS: the lack of states localized in site *C*, around $E = \pm 1$ eV, as showed by the green/triangle points in the right lower panel of Fig. 3.

In summary, for systems with an even number of sites, in a tight binding approach and with an energy-independent model approximation for the self-energy, we have a valley in the transmission function for these systems (E1 and E3) with an exception for a symmetric system containing an odd number of sites (system E2) on each possible branch (upper and lower pathway) of the system. Let’s see how things works for systems with odd number of total sites.

4.2 Odd systems

The results for the transmission function and the LDOS, for systems containing an odd number of total sites are depicted in figure 4, in the upper and lower panels, respectively. Once more, let’s remind that for a 2T-device, if the Fermi level (E_F) coincides with the

onsite energy ($E_F = \lambda_0$), the systems with an odd number of sites have a peak in the transmission function when $E = E_F = \lambda_0$ [2,13].

Starting from the system O1, we can see in the left upper panel of figure 4 that for this system a peak in the transmission function for $E=0$ occurs for both pathways, i.e., for T_{AB} (red/full line) and for T_{AC} (black circles), as expected. Similar to some even systems, this system is also symmetric, not only in the sense that the upper and the lower pathways are equal, resulting in $T_{AB}(E) = T_{AC}(E)$, but also in a topological sense, once the LDOS are identical for all renormalized sites. Note that system O1 has an odd number of total sites (seven sites) and also an odd number of sites on each possible pathway five sites from site *A* to the site *B* and the same from site *A* to site *C*. However, if for seven sites in a tight binding approach, seven eigenvalues are expected, we can see that only five peaks appear in the transmission function. This feature can be understood analyzing the LDOS (lower left panel) of the system O1 where we can see degenerate states delocalized through all the system, around the values $E = \pm 1$ eV, explaining the existence of only five transmission's peaks. Thus, similar to the even cases, we can see that an odd 3T-system containing two odd branches, behaves like an odd 2T-system containing the same number of sites of each branch of the 3T-system.

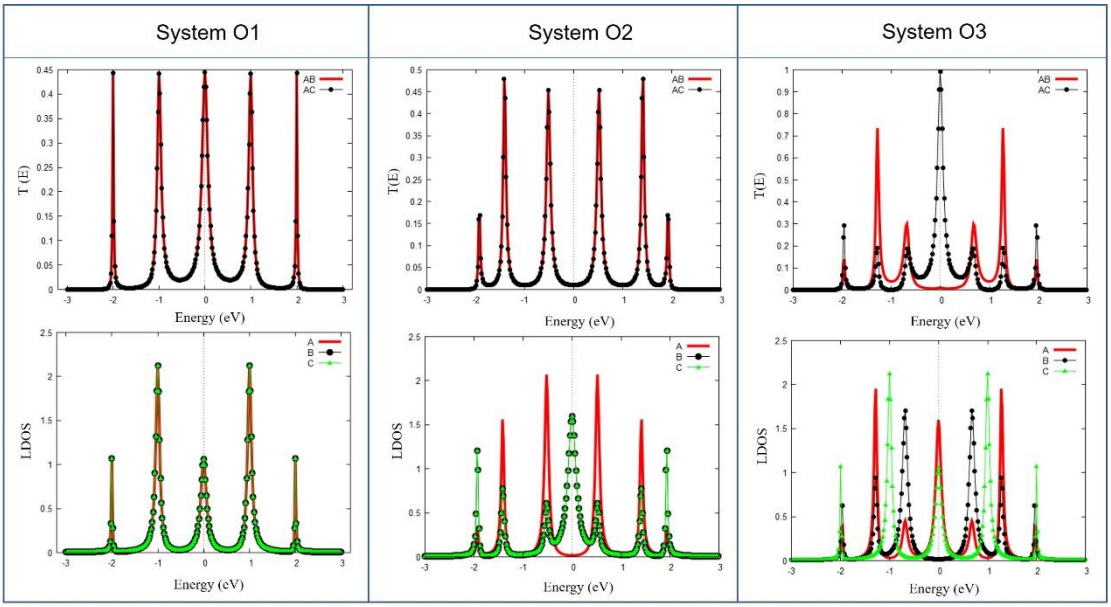

Figure 4: Transmission (upper panels) and LDOS (lower panels) for the three studied odd systems. For transmission (upper panels), red/full line is the transmission from site A to site B and the black circles, the transmission from site A to site C. For LDOS (lower panels) we have: red line, black circles and green triangles as the LDOS curves in sites A, B and C, respectively.

For system O2, things are somewhat different and a valley in the transmission function can be observed at $E = 0$ eV as showed in the upper central panel of Fig. 4. In spite of the total number of sites being odd, the main feature in this case is the even number of sites on each pair of symmetric pathways. The consequence of this feature in the behavior of the transmission function can be understood analyzing the LDOS (lower central panel) of the system O2, where is evident an absence of a localization in site A, for the state with λ

= 0 eV, as shown by the red/full line. As a consequence, around E = 0 eV, we have a forbidden transport channel and we can conclude that an odd 3T-system with two even branches, behaves like an odd 2T-system containing the same number of sites of each branch of the 3T-system.

Finally, we have the asymmetric system O3, containing a total of seven sites and with the upper pathway (from site *A* to site *B*) having an even number of sites (six sites) and from *A* to *C* (lower branch) an odd number of sites (five sites). As in the case of system E3, the difference between the upper and the lower pathways brings an asymmetric behavior in the transmission function, i.e., $T_{AB}(E) \neq T_{AC}(E)$, as showed by the full red line and the black circles in the upper right panel of figure 4. Note that, while for the lower pathway, with an odd number of sites, we have a peak in the transmission function ($T_{AC}(E)$) at E = 0 eV, for the upper pathway, with an even number of sites, we have a valley in the transmission at E = 0 eV. So, in principle, each branch behaves like their 2T-sytem analogs. Once more, this difference in the transmission can be explained by the LDOS: the lack of a state localized in site *B*, around E = 0 eV, suppress a peak transmission for the even upper even-pathway ($T_{AB}(E)$) as showed by the black/circle points in the right lower panel of Fig. 4. Note that the opposite behavior can be found for lower odd-pathway where at E = 0 eV a state localized at both sites *A* and *C* exist, as showed in the lower right panel of Fig.4, by the red/full line and the green/triangle points.

4.3 Electrical Current

In obtaining the electrical currents curves showed in figures 5(a-d), some approximations were made: small temperature such that the Fermi function can be approximated by a step function, a symmetric applied voltage (V_{ap}) between left (contact *S*) and right contacts (contacts *U* and *D*), i.e., $V_A = -V_{ap}/2$ and $V_B = V_C = +V_{ap}/2$ (see Fig. 1) and the bias voltage drops occurs only at the contact-device interface. Also, we will plot the dimensionless ratio I_{AX}/I_0 ($X = B, C$) instead of I_{AX} with: $I_0 = 2e\delta/h$ and δ=1 *eV*.

Figures 5(a-d) show the electrical currents (see Eq. 9) for all six systems studied. Roughly speaking, we can correlate the plateaus, marked with dash lines and with corresponding colors, to the valleys of the transmission function of Figs. 3 and 4. Moreover, in some cases (systems *E1*, *E2*, *O1* and *O2*), the transmissions are symmetric, in the sense that the upper pathway (from site *A* to site *B*) has an equal transmission when compared to the lower pathway (from site *A* to site *C*), i.e., $T_{AB} = T_{AC}$. Thus, once by Eq. 9 when$T_{AB} = T_{AC}$ then, necessarily, we will have $I_{AB} = I_{AC}$ and, in these symmetric cases, to understand the electrical current curve, it's enough analyze only I_{AB}.

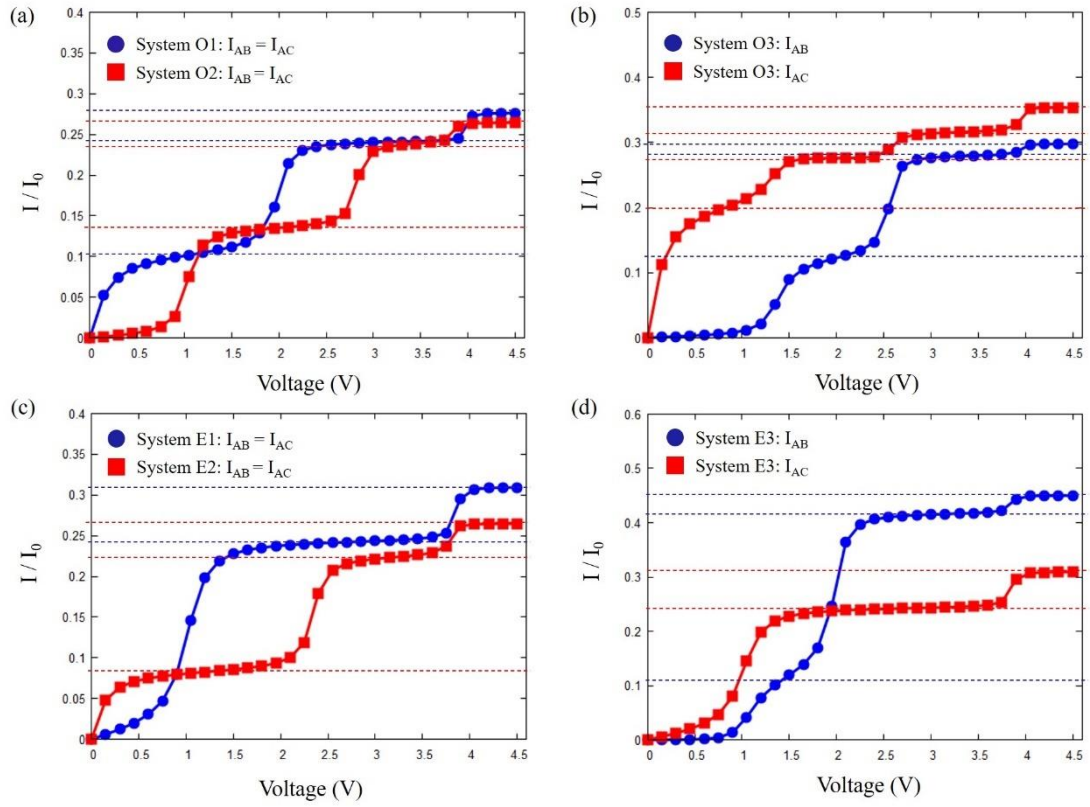

Figure 5:Electrical current (divided by I_0) for the six systems. In (a) we plot only I_{AB} for even systems (E1 and E2) once by symmetry we have $I_{AB}= I_{AC}$. In (b), the curves I_{AB} and I_{AC} for the asymmetric system E3. In (c) we plot only I_{AB}, once by symmetry, for even systems (E1 and E2) we have $I_{AB}= I_{AC}$ and in (d) the curves I_{AB} and I_{AC} for the asymmetric system O3. Dashed lines indicate the plateaus.

Starting from the symmetric odd cases, in Fig. 5a, for example, we have for system *O1* that the current (blue circles) starts immediately after the voltage is turn on and around V_{ap} = 1 V we have a middle point of a plateau. A new jump in the electrical current can be observed around V_{ap} = 2 V and a new plateau appears with its middle point around V_{ap} = 3 V. Finally, a little jump in the current appears around V_{ap} = 4 V and subsequently, we have a new little plateau just after this voltage value. Comparing the previous information with the left upper panel of Fig. 4, we can see that exactly at the (symmetrical) values of energy given by $E = \pm eV_{ap}/2$ (with e =1), a valley exists in the transmission function. This fact, permit us associate these valleys to the plateaus and the peaks in transmission to the jumps of the electrical currents. Thus, applying the same reasoning for the system *O2* we have three plateaus, with middle points located around: V_{ap} = 2.0 V, V_{ap} = 3.5 V and V_{ap} = 4.5 V, respectively. Note that, for each value of energy given by $E = \pm eV_{ap}/2$, i.e., at E = ±1.0 eV, E = ±1.75 eV and E = ±2.25 eV, a valley exists in the transmission function for system *O2* as depicted in the upper central panel of Fig. 4. Also, the jumps in the electrical current curve can be identified with the peaks of the transmission function: peaks [jumps] at E = ±0.5 eV [V_{ap} = 1.0 V], E = ±1.5 eV [V_{ap} = 3.0 V] and E = ±1.9 eV [V_{ap} = 3.8 V]. By inspection, is straightforward to see that all other curves of electrical current, can be interpreted with the same reasoning.

5. CONCLUSIONS

In this work we study the quantum coherent transport through six different devices composed by a linear chain with three terminals, adopting a tight binding approach, to simulate the semi-infinity contacts, and using decimation techniques to renormalize the system, in order to be treated analytically. In particular, it was analyzed how even-odd effects change the behavior of the transmission function of these systems, as function of the parity of the total number of sites and number of sites of each branch. Despite simple, this model is capable to show the main trends for this kind of systems, as reported by many authors [15–17,20].

In the case of odd-systems, we show that a simple rule similar to the 2T-systems with odd number of sites, can be obtained: the presence of a peak in the transmission function at $E = E_F$ for each branch of the system containing an odd number of sites. For even-systems, symmetry considerations must be taken account. In general, for even-systems we have a valley in the transmission function at $E = E_F$ – like in systems *E1* and *E3* – unless we have a symmetric system containing an odd number of sites on each possible branch, as in system *E2*. In this case, we have a presence of degenerate delocalized levels at $E = E_F$ giving rise to a peak in the transmission at this energy value. The transmission functions behaviors explain the shapes of the electrical current curves: if we exclude the valley at $E = E_F = 0$ eV in case it appears in the transmission function at this energy point, each valley will give rise to a plateau in the electrical current curve. However, for the present case, due to the symmetry in the applied voltage, the number of plateaus above $I_{AB} = 0$ (and $I_{AC} = 0$) will correspond to a half of number of valleys in the transmission function, again excluding the valley at $E = 0$ eV.

The above features can bring some possibilities for applications of these kind of systems. For example, once the electrical and thermal conductance in the zero-temperature limit and small applied voltages, depend of the transmission function at the Fermi energy [27–29], based in even-odd effects in 3T-devices, one can design electronic components at nanoscale based on the parity behavior of these systems. For the moment this purpose is out of the scope of the present work, but certainly will be explored in future works.

Acknowledgments: This research was carried out with financial support from Federal University of Pernambuco (Brazil). L. Marques acknowledge the financial support of the Portuguese Foundation for Science and Technology (FCT) in the framework of the Strategic Funding UIDB/04650/2020 and projects SATRAP (POCI-01-0145-FEDER-028108), SATRAP+(EXPL/FIS-MAC/0947/2021). The authors also acknowledge the Texas Advanced Computing Center (TACC) at The University of Texas at Austin for providing access to STAMPEDE2 - HPC resources that have contributed to the research results reported within this paper.

6. *REFERENCES*

1. Aviram, A. & Ratner, M. A. Molecular Rectifiers. *Chem. Phys. Lett.* **29**, 277–283 (1974).
2. Juan, E. S. & Carlos Cuevas. *Molecular Electronics: An Introduction to Theory and Experiment*. vol. 1 (Word Scientific, 2010).
3. H. -S. Sim, H. -W. Lee & K. J. Chang. Even-odd behavior of conductance in monatomic sodium wires. *Phys. Rev. Lett.* **87**, 4 (2001).
4. Rafael Gutiérrez, Frank Grossmann & Rüdiger Schmidt. Resistance of Atomic Sodium Wires. *Acta Phys. Pol. B* **32**, 7 (2001).
5. Georg Heimel, Lorenz Romaner, Jean-Luc Bredas & Egbert Zojer. Odd-Even Effects in Self-Assembled Monolayers of ö-(Biphenyl-4-yl)alkanethiols: A First-Principles Study. *Langmuir* **24**, 9 (2008).
6. George M. Whitesides *et al.* Odd-Even Effects in Charge Transport across Self-Assembled Monolayers. *J Am Chem Soc* **133**, 14 (2011).
7. Jiangni Yun *et al.* Interesting Odd-Even Effect, Ohmic Contact, Negative Differential Resistance,and Current Stabilizer Behavior in All-Carbon Graphyne/Carbon-Chain Junctions. *IEEE Trans. ELECTRON DEVICES* **67**, 7 (2020).
8. Tal Toledano *et al.* Odd−Even Effect in Molecular Electronic Transport via an Aromatic Ring. *Langmuir* **30**, 10 (2014).
9. Hylke B. Akkerman *et al.* Effects of Odd−Even Side Chain Length of Alkyl-Substituted Diphenylbithiophenes on First Monolayer Thin Film Packing Structure. *J Am Chem Soc* **135**, 9 (2013).

10. M. Qiu, K. M. L. Odd−Even Effects of Electronic Transport in Carbon-Chain-Based Molecular Devices. *J Phys Chem C* 5 (2012) doi:dx.doi.org/10.1021/jp300073t.
11. P. Havu, T. Torsti, M. J. Puska & R. M. Nieminen. Conductance oscillations in metallic nanocontacts. *Phys. Rev. B* **66**, 5 (2002).
12. R. H. M. Smit, C. Untiedt, G. Rubio-Bollinger, R. C. Segers & J. M. van Ruitenbeek. Observation of a Parity Oscillation in the Conductance of AtomicWires. *Phys. Rev. Lett.* **91**, 4 (2003).
13. Nozaki, D., H M Pastawski, & G Cuniberti. Controlling the conductance of molecular wires by defect engineering. *New J. Phys.* **12**, 20 (2010).
14. Di Ventra, M. *Electrical transport in nanoscale systems*. (Cambridge University Press, 2008).
15. Mardaani, M., Rabani, H. & Esmaeili, A. An analytical study on electronic density of states and conductance of typical nanowires. *Solid State Commun.* **151**, 5 (2011).
16. J. H. Ojeda, R. R. Rey-González & D. Laroze. Quantum transport through aromatic molecules. *J. Appl. Phys.* **114**, 8 (2013).
17. Pastawski, H. M., Cattena, C. J., J Fernándes-Alcázar, L., Bustos-Marún, R. & Nozaki, D. Generalized multi-terminal decoherent transport: recursive algorithms and applications to SASER and giant magnetoresisteance. *J Phys Condens Matter* **26**, 14 (2014).
18. Thomas M. Henderson, Giorgos Fagas, Eoin Hyde & James C. Greer. Determination of complex absorbing potentials from the electron self-energy. *J. Chem. Phys.* **125**, 10 (2006).
19. Ojeda, J. H., Laroze, D. & Orellana, P. A. Aromatic molecules as spintronic devices. *Jounal Chem. Phys.* **140**, 6 (2014).

20. Davison, S. G. & Kucharczyk, R. Effect of molecular wires attached to benzene: Local density-of-states study. *Phys. Rev. B* **69**, 8 (2004).
21. Datta, S. *Quantum transport: atom to transistor*. (Cambridge University Press, 2005).
22. Yonatan Dubi. Transport Through Self-Assembled Monolayer Molecular Junctions: Role of In-Plane Dephasing. *J Phys Chem C* **118**, 9 (2014).
23. Bingqian Xu & Yonatan Dubi. Negative differential conductance in molecular junctions: an overview of experiment and theory. *J. Phys. Condens. Matter* **27**, 19 (2015).
24. Maiti, S. K. Multi-terminal quantum transport through a single benzene molecule: Evidence of a molecular transistor. *Solid State Commun.* **150**, 6 (2010).
25. C. J. O. Verzijl, J. S. Seldenthuis & J. M. Thijssen. Applicability of the wide-band limit in DFT-based molecular transport calculations. *J. Chem. Phys.* **138**, 11 (2013).
26. Datta, S. *Electronic transport in mesoscopic systems*. (Cambridge University Press, 1995).
27. J C Cuevas, J Heurich, F Pauly, W. Wenzel & Gerd Schon. Theoretical description of the electrical conduction in atomic and molecular junctions. *Nanotechnology* **14**, 10 (2003).
28. Datta, S., Ratner, M. A. & Xue, Y. First-principles based matrix Green´s function approach to molecular electronic devices: general formalism. *Chem. Phys.* **281**, 20 (2002).
29. Yifan Li, J. L., Hui Li, J. D. H. & Yi Zhou. Electronic transport properties of carbon and boron nitride chain heterojunctions. *J. Mater. Chem. C* **5**, 14 (2017).